Convento dos Capuchos Mortars' Analysis

Bernardo Rodrigues Mendonça Aguiar de Matos

Department of Civil Engineering, Architecture and Georesources, Instituto Superior Técnico, Universidade de Lisboa

Abstract: The Convent of the Capuchos was founded in 1560, to house a Franciscan order in the Pena's top. Stripped of luxury goods, the monks lived in the Convent built using the outcrops of granite rocks as walls, small spans, narrow aisles and very small cells.
Parques de Sintra – Monte da Lua, S.A is currently the entity in charge of the management, control, conservation and restoration of the Covent that is integrated in the Cultural Landscape of Sintra listed as World Heritage by UNESCO.
The article characterizes a set of mortar samples collected in different zones and compartments of the Convent with the objective of contributing for the existing knowledge regarding the materials present in the Convent and to support the formulation of replacement mortras in the future.
The historic mortars' characterization took place in the DECivil laboratory, at Instituto Superior Técnico. The implemented methodology was based on the study of the mortars' physical properties, colorimetric characterization, aggregate characterization and binder/aggregate ratio.
Most samples showed results associated with the characteristics of historical mortars, from composition, granulometry to behavior in contact with water. However, one of the samples showed different results, comparable to a more recent mortar.

Keywords: Convent of the Capuchos – Mortars – Composition – Characterization

1. Introduction

The Convent of the Capuchos is located in Serra de Sintra, namely in the parish of Colares, east of Cabo da Roca towards Pena, located in the Sintra-Cascais natural park. The Convent is integrated in the Cultural Landscape of Sintra listed as World Heritage by UNESCO (UNESCO, 1995).

Built in the 16th century to house a Franciscan order, the Convent of the Capuchos is a property that represents a historical and religious testimony. With several owners over time, the information regarding past interventions are almost inexistent, only some information was found regrading interventions carried out by DGEM. Over time, abandonment and vandalism actions deteriorated the Convent.

Since ancient times, lime has been used as construction material, starting with the Greek civilization, even before Christ, until the Roman Empire, making up eight centuries of utilization of this technology (Veiga, 2006).

The historic mortar's present several characteristics inherent to its time, location and building typology. Old mortars can include white lime nodules, with different dimensions, fibers, oils, ash or even ceramic materials (Damas et al., 2016; Veiga, 2018).

The cement mortars are not compatible with those of lime, having been found lower durability levels in most cases (Veiga, 2006). Therefore, it is even more of paramount importance that used materials are known in detail. In Portugal, it is still an underexplored domain, too case-by-case, but it is essential for the study of viable solutions that do not undermine the heritage value (Appleton, 2011).

The mortar's characterization is started by searching the time, traditions and building technicalities utilized. The typology, the purpose with which was conceived and the climatic conditions are also important information to gather. Not only on a general perspective, but also on the sample perspective, it is crucial to understand the mortar's function, the number of layers, the binder:aggregate ration and its components. Finally, one should assume as a base criteria of an old sample analysis that its initial conditions will not be found anymore (Damas et al., 2016).

An in-depth and multidisciplinary research includes also the chemical, mineralogical, petrographic and physical characterization of the mortars. This analysis leads, for example, to the knowledge of the types of materials (sands, ceramic powder, gravel) used in the mortars and organic additives that may have been added (Appleton, 2011).

1.1. Old Mortars – Characteristics and Composition

The renders sometimes have considerable dimensions, greater than 5 centimetres in its total thickness, to overcome the irregularity of the supports. The old renders are usually made of more than one mortar layer with different compositions, ensuring a binder reduction as one moves away from the support.

The execution was designed from the inside to the outside, with the innermost layer (roughcast) being the one with the greatest resistance and connection to the surface. Therefore, it is the most susceptible to shrinkage and cracking. This layer application was interspersed

with the next one to ensure drying time, hardening and to undermine the potential risk of cracking. The next layers (plaster), weaker than the first due having less binder, turns out to be a smoothing layer. Lastly, the final layer (plaster mortar) has a protection function of the others, finishing and decoration (Appleton, 2011; Veiga, 2006).

The old mortars can be quite diverse in terms of composition and constituents. The total span of binder:aggregate ratios by mass is between 1:1 and 1:4: values from 1:1 to 1:2.5 are more common in mortars richer in lime, while the poorest present a range between 1:2.5 and 1:4. This as related to the building importance, namely traces richer in binder have origin in samples from palaces, military and even religious constructions (Veiga, 2017, 2018).

Lime nodules are commonly detected in old mortars and can be the result of flocculation and water trapping in the lime particles, preventing their good hydration and subsequent carbonation (Gomes et al., 2013).

The uses of natural additives in old mortars, sometimes with pozzolanic properties, has been frequently reported. Vitrúvio reported that mixing ashes from Mount Vesuvius with lime resulted in strength gains as wells as hardening under water, and consequently, conferring hydraulicity to the lime (Aicher et al., 2001). Organic additives, fibers and fats were also used in the formulation of these mortars due to its air-introducing characteristics, promoting lime carbonation (Veiga, 2017).

The aggregate's choice directly influences the final strength of the mortars, as differences in aggregate porosity have a direct impact on the CO_2 diffusion throughout the sample. Therefore, higher levels of porosity are related to higher carbonation rates, and consequently, more favourable conditions for the setting of lime based mortars (Scannell et al., 2014).

In old mortars, the aggregates used are mostly of natural origin, thus their geometry and granulometry are typically dependent on the local geology. (Lezzerini et al., 2014).

The aggregate properties are relevant, not only because it is the mortar skeleton, but also because its locations, shape, granulometry and porosity influence the final product. For example, a well graded aggregate reduces the voids volume as well as it promotes carbonation – a good graded mixture separates lime particles, facilitating carbonation and decreasing the probability of lime nodules presence (Margalha et al., 2007). On the other hand, a graded mixture, but rich in clay, jeopardizes a good bond between the binder and larger aggregates, creating a loss of adhesion and consequently a strength loss (Huaracha, 2018; Margalha et al., 2007).

1.2. Physical characterization

In general, old mortars are characterized by having high porosity and permeability, which affects other physical properties,their mechanical behaviour and durability. The total porosity, pore size distribution and specific surface are properties of with relevance to the final structure description, and consequently, influences all these characteristics (Groot, 2005).

The amount of water needed for the formulation is only dependent of the desired consistency and workability conditions. As previously mentioned, the added water is not consumed during reaction processes and, with its evaporation over time, empty spaces are created which are determinant for porosity in its hardened state (Gomes et al., 2013).

Considering that aggregates often have lower porosity levels than the mortar binder, their characteristics play a determining role in the overall mortar physical conditions. Lime nodules that can have an important presence in old mortars, as mentioned above, can contribute to a significant increase in porosity and water retention capacity.

According to Veiga (2009), mixes with higher lime content present higher porosity values and capillarity coefficients. For this reason, the binder/aggregate ratio variability, as well as additives, contribute to improve some characteristics of aerial lime mortars. These values may also be compared with aerial lime mortar formulations produced in the laboratory. Table 1 shows some values obtained by two different references, with the objective of comparing the physical properties of mortars with those that were laboratory formulated.

Table 1 Physical characteristics of old and laboratory-produced mortars.(Garijo et al., 2020; Veiga, 2018).

Physical Characterization				
Ref.	**Ratio**	**Open Porosity**	**Capillarity coeff.**	**Apparent Density**
(Veiga, 2018)	**w/b**	**[%]**	**[kg/m^{2}s^{0,5}]**	**[kg/m^3]**
	1:3	27 - 35	0,14 – 0,31	1780
	1:2	28 - 39	0,25 – 0,36	1800 - 1830
	1:1	34 - 35	-	-
(Garijo et al., 2020)	1:1/1,25	25 - 30	0,14 – 0,21	1800 - 2000

Comparing the 2 studies, the laboratory results of Garijo et al. (2020), show similar values in apparent density to those of old mortars from Veiga (2018), but slightly lower in the other. The moulds used in the tests were metal and wood made, to simulate a damp brick masonry wall. In the metal moulds, there were lower porosity results, however, those with porosity improvements and a decrease in the Capillary Coefficient, it focused on the use of crushed limestone aggregate compared to river bed – it improved the cohesion between the particles inside the mortar and the crystallographic bond between aggregates and aerial lime (Garijo et al., 2020).

1.3. Mechanical characterization

The collection and characterisation of old mortar samples need to consider their function, whether it is rendering, bedding or paiting mortar (Ferreira Pinto et al., 2020; Groot, 2005).

Usually, aerial lime mortars are characterized by their reduced mechanical strength, especially compared to

cementitious mortars, and they have an interesting behaviour when facing some deformations imposed by masonry movements (Huaracha, 2018).

The mortar strength gain with aerial lime occurs by carbonation, thus the presence of an exaggerated amount of water can delay the initial setting (Gomes et al., 2013). and contribute for an increased presence of voids (Huaracha, 2018). In summary, higher porosity values are related to the increase in the mortar permeability, and consequently, with low durability values that imply a weaker mechanical strength (Nogueira, et al., 2016).

Excessive water, combined with high humidity conditions, can create an environment conducive to the formation of lime nodules. The nodules are punctual areas in with there is flocculation and water trapping by the lime particles, preventing their good hydration and subsequent carbonation. The greater the lime nodules number, the lower the conditions for agglutination and increased in the satisfactory mechanical strength of the mortar (Gomes et al., 2013; Sena da Fonseca et al., 2020).

During the drying and hardening process of lime mortars, cracks usually appear. However, the plasticity and slow carbonation of these mortars contribute to these cracks being able to close. The phenomenon occurs due to the partial dissolution of calcite that may exist, which, when exposed to infiltrated water retained in the voids, triggers a recrystallization process (Sena da Fonseca et al., 2020; Veiga, 2017).

The aggregate choice also impacts the mechanical strength. If the used aggregate has low mechanical strength, it is likely that the mortar will break through the aggregate. On the other hand, aggregates with high mechanical strength may cause ruptures at the binder/aggregate interface, assuming by hypothesis that the aggregate is stronger than the binder (Scannell et al., 2014).

The used aggregates may not have the correct granulometry so the line favors compactness. Porosity is the mortar characteristic that most propagates the various associated weaknesses and that typically most influences its mechanical strength (Nogueira et al., 2016; Veiga, 2018).

According to Scannell et al. (2014), previous studies analysed the evidence of increased mechanical strength in mortars, where the aggregate used showed mineralogical similarities with the binder. Therefore, the combination of limestone aggregate may form a more favorable agglutination for the final gain in mortar strength, compared to the use of silicate aggregate when dealing with lime based mortars.

Table 2 presents some values obtained in the scope of three research works, with the aim of comparing the mechanical properties of old mortars ((Silva et al., 2010), (Appleton, 2011) and those formulated in the laboratory (Garijo et al., 2020).

Table 2 Mechanical characterization of mortar samples.

Mechanical characterization			
Reference	**Compression Strength [Mpa]**	**Traction Strength [Mpa]**	**Flexibility module [Mpa]**
(Silva et al., 2010)	2,0 – 3,6	-	-
(Appleton, 2011)	0,4 – 2,5	0,2 – 0,7	2000 - 5000
(Garijo et al., 2020)	0,6 – 1,5	0,3 – 0,55	2250 – 2750

2. Experimental characterization

2.1. Samples

The studied mortar samples were collected by PSML from different constructive elements of the Convent of the Capuchos. After being collected, the samples were subject to a visual description and to photographic records. In the DECivil laboratory at IST, the samples were characterised.

On the first level of the Convento dos Capuchos, three samples were collected at Capela da Paixão (designated as CPE1, CPE2 and CPE3), one at the Herbolário (designated as HE1) and one at the main entrance (designated as GA1). On the second level of the Convent, samples were collected from four different locations: kitchen, area next to pavement (designated as CZ1); cell nº 3 in the cell corridor (designated as CE1); water house, next to the pavement under the small span (designated as CA1); and in the Chapter Room (designated as ASC1). Tables 3 and 4 summarize the characteristics of the mortar samples.

2.2. Test Methods

The mortars characterization included a macroscopic physical characterization and parameters related with typology, morphology, cohesion, lime nodules presence, voids occurrence, and biocolonization were defined. Then, a spectrocolorimeter was used to obtain the CIELAB coordinates. These coordinates were create on the assumption of constantly correlating colour values with visual perception, using the assumption that the same colour cannot be any primary colour or a colour conjugation, at the same time (Minolta, 2014). In figure 1, a representation of the three-dimensional space created by the coordinate system can be seen.

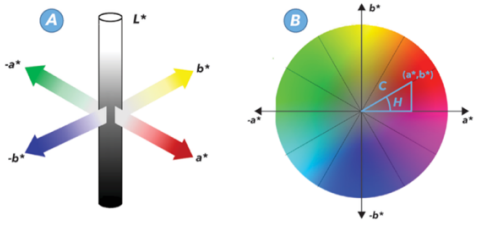

Figure 1 Three-dimensional color space according to CIELAB. Adapted from (Delazio et al., 2017).

The determination of open porosity was performed according to the procedures of RILEM Test No. I.1(25-PEM - Protection et Érosion des Monuments, 1980a). To

start the test, the samples were placed in a ventilated oven to be dried at a constant temperature of 60º Celsius, with allowed variations of +/- 5º Celsius.

Real density refers to the proportion of mass with impermeable volume, in kilograms per cubic meter [Kg/m^3]. To obtain the impermeable volume, the saturated sample must be weighed and the mass of the pore space accessible to water subtracted.

To determine the water content after 48 hours of water immersion, the samples were placed in a ventilated oven at 60º Celsius, with allowed variations of +/- 5º Celsius, for 2 hours. Afterwards, the samples were removed and weighed to obtain their dry mass, M_{dry}. Subsequently, samples were immersed in water for 48 hours to obtain the saturated mass, M_{sat}. Finally, the saturation coefficient, C_{sat}, is the ratio between the water content after 48 hours of immersion and the maximum water content. This reason allows us to verify the ease of samples saturation, being another indicator that complements the analysis of the behaviour of samples in the presence of water (Almeida Santos, 2013).
The capillary water absorption coefficient determination was performed according to the procedures described in RILEM Test No. II.6 (25-PEM - Protection et Érosion des Monuments, 1980b). The samples were placed inside a container with an approximately 2mm film of water. To promote the absorption water, these were placed in individual baskets whose base had a geotextile.

The binder: aggregation ratio was estimated using the acid etching of mortar samples, since the visual observation made it possible to verify the presence of siliceous aggregate. Otherwise, this technique use would dissolve not only the binder but also the carbonated aggregater, undermining the desired effect: considering the soluble part as the binder and the insoluble aggregator (Antunes & Coroado, 2013; De Carvalho Antunes et al., 2016; Sena da Fonseca et al., 2020).

A diluted hydrochloric acid solution was prepared, in the proportion of 2mol/dm^3 in which 500ml of the HCL solution was used for 50g to 70g of the sample. The binder was dissolved and the remaining solid residue corresponds to the aggregate (Rosa, 2016). Afterwards, it was performed a careful filtration to obtain the fines mass retained on the filters, which were placed to dry in an oven. Finally, from the ratio exemplified in the equation 1, it is possible to estimate values of the soluble/insoluble residue of each sample.

$$ratio = \frac{M_{soluble}}{M_{insoluble}} = \frac{M_{binder}}{M_{aggregator}} \quad [1]$$

Then, there was the aggregator characterization by sieving. The sieves series used corresponds to the size ranges: 4mm, 2mm, 1mm, 500µm, 250µm, 125µm, 63µm, and <63µm.

After cleaning, individual weighing and assemble of the whole series of sieves, the sample is introduced, and sieving can be started. The mass that crosses all meshes and is retained at the base, corresponds to the dimension of aggregate smaller than <63µm.

The thinness modulus (MF), maximum dimension (D_{max}) and minimum dimension (D_{min}) of the aggregate are properties inherent to each sample and improve its characterization. D_{max} is defined as the smallest opening of the sieve in the series used where at least 90% of the sample mass has passed.

D_{min} corresponds to the largest sieve opening of the series through which no more than 5% of the sample mass passes. The thinness modulus corresponds to the division by 100 the sum of the retained sample of each sieve. D_{60} D_{30}, and D_{10} corresponds to the size such 60%, 30% and 10% are finer than. With this 3 size parameters is possible to calculate the coefficient of curvature (C_c) and coefficient of uniformity (C_u) .

Table 3 Photographs of the mortar samples.

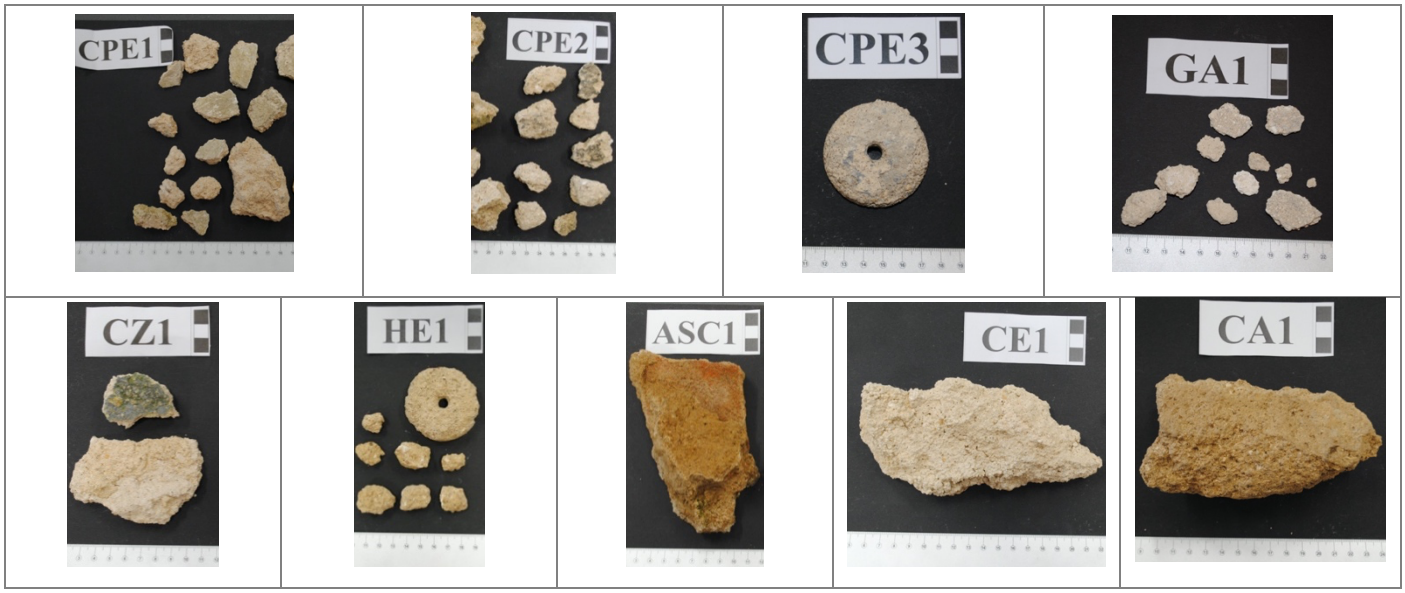

Table 4 Summary table of the visual description of the samples: +++: high; ++: medium; +: low; -: residual or without occurrence.

Nº Frag	20		Nº Frag	26		Nº Frag	1	
Colour	Beige		Colour	Beige and grey		Colour	Beige, grey, brown	
Cohesion	Medium		Cohesion	Low		Cohesion	High	
Lime Nodules	++		Lime Nodules	-		Lime Nodules	+	
Bioc.	+		Bioc.	+		Bioc.	-	
Type	Render		Type	Render		Type	Render	
Nº Frag	11	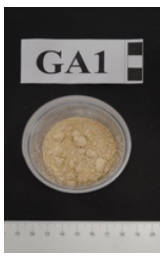	Nº Frag	13		Nº Frag	8	
Colour	Light beige		Colour	Grey, beige		Colour	Beige, grey	
Cohesion	Very low		Cohesion	Low		Cohesion	Medium/ Low	
Lime Nodules	++		Lime Nodules	++		Lime Nodules	+++	
Bioc.	-		Bioc.	+		Bioc.	++	
Type	Render		Type	Render		Type	Render	
Nº Frag	8		Nº Frag	2	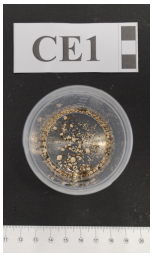	Nº Frag	1	
Colour	Dark Beige, grey		Colour	Beige		Colour	Dark Beige	
Cohesion	Medium		Cohesion	Medium		Cohesion	High	
Lime Nodules	-		Lime Nodules	+++		Lime Nodules	++	
Bioc.	+++		Bioc.	+		Bioc.	-	
Type	Render		Type	Render		Type	Render	

3. Results and discussion

3.1. Macroscopic Description

GA1, CPE1, CPE2 and CZ1 samples included several mortar fragments with diverse dimensions. ASC1, CE1 and HE1 samples included a reduced number of mortar fragments. CPE3 and CA1 samples correspond each one of just one mortar fragment, both bigger than the previous.

Regarding the biocolonization present in the samples, samples GA1, CPE3 and CA1 were the ones that required lighter cleaning, as they did not show signs of biocolonization. The rest were all subjected to careful cleaning.

The presence of lime nodules with diverse dimensions was notorious in most samples, except for the ASC1 and CPE2 samples. In samples CE1 and CZ1, the visual observation noticed not only the presence of nodules but also a more relevant presence of voids in comparison with the other tested samples.

Sample CA1 distinguished itself from the others, since it integrated two layers of mortar – an outer layer more cohesive of about 4 cm and an inner layer with less cohesion and greater number of lime nodules with different dimensions.

3.2. Composition and aggregate grading

Regarding the mortars composition, the binder:aggregate (b:a) composition estimated based on the soluble and insoluble residues are in the range of 1:2 and 1:4, table 5.

Table 5 Binder:aggregate rations by mass and grading parameters of the aggregates.

Sample	b:a	MF	$D_{máx}$ [*mm*]	D_{min} [*mm*]
CPE1	1:2,3	4,36	4	<0,063
CPE2	1:2	4,18	4	<0,063
CPE3	1:6,2	5,27	4	0,125
GA1	1:2,4	4,27	2	<0,063
CZ1	1:3,3	4,36	4	<0,063
HE1	1:4	4,29	2	<0,063
ASC1	1:2,4	4,66	4	<0,063
CE1	1:3,5	4,28	4	<0,063
CA1	1:2,8	3,93	2	<0,063

The outside samples, namely CPE1, CPE2 and ASC1, revealed a b:a value of around 1:2 associated with render mortars (Appleton, 2011; Veiga, 2018). According Damas et al.(2016), HE1 showed trace value associated with plaster mortar. Regarding CPE3, the value of the b:a fits the value of the render mortar associated with a military building.

CA1 and CE1 samples showed very similar values, with CE1 showing a lower binder content. However, the trace value obtained from CA1 is closer to a render mortar while CE1 in a plaster mortar.

Finally, the CZ1 sample presented a b:a value of 1:3.3 which is not unreasonable to associate with a plaster mortar.

Additional data for the samples granulometry characterization, namely fineness modulus, D_{max}, D_{min}, D_{60}, D_{30}, D_{10}, C_u and C_c of the aggregates can be seen in table 5 and 6. Particle size distribution of the aggregates from samples can be seen at figure 2.

Table 6 parameters calculated from particle size distributions.

Sample	D_{60} [*mm*]	D_{30} [*mm*]	D_{10} [*mm*]	C_u	C_c
CPE1	0,78	0,16	0,073	10,6	0,5
CPE2	0,70	0,14	n.d.	n.d.	n.d.
CPE3	1,19	0,63	0,261	4,6	1,3
GA1	0,71	0,24	0,065	10,9	1,3
CZ1	0,82	0,20	n.d.	n.d.	n.d.
HE1	0,79	0,20	0,064	12,2	0,8
ASC1	0,99	0,31	0,080	12,3	1,2
CE1	0,77	0,17	n.d.	n.d.	n.d.
CA1	0,49	0,15	n.d.	n.d.	n.d.

At first, it is denoted that CPE2, CZ1, CE1 and CA1 samples did not present particle sizes whose percentage met D_{10}. Therefore, the curvature coefficient and samples uniformity remain undefined.

Fineness modulus figures ranged between 3.93 and 5.27, D_{min} is <0.063mm in all samples, except CPE3 which revealed 0.125mm, and D_{max} ranged between 2 and 4mm. The curvature coefficient presented values between 0.5 and 1.3, while uniformity coefficient was between 4.6 and 12.3.

According to the Unified Soil Classification, such as the $C_u > 3$ and $1 \leq C_c \leq 3$, it can be considered that the aggregated have a well graded sand classification.

Regarding the curves' particle size represented in figure 5.12, three curves differ from the others: CPE3, ASC1 and CA1. CPE3 showed the highest values of fine modulus and D_{min}, representing the samples with the largest particles, while CA1 was the sample whose particles showed the smallest dimensions. ASC1 had the C_u highest value, being considered medium uniform.

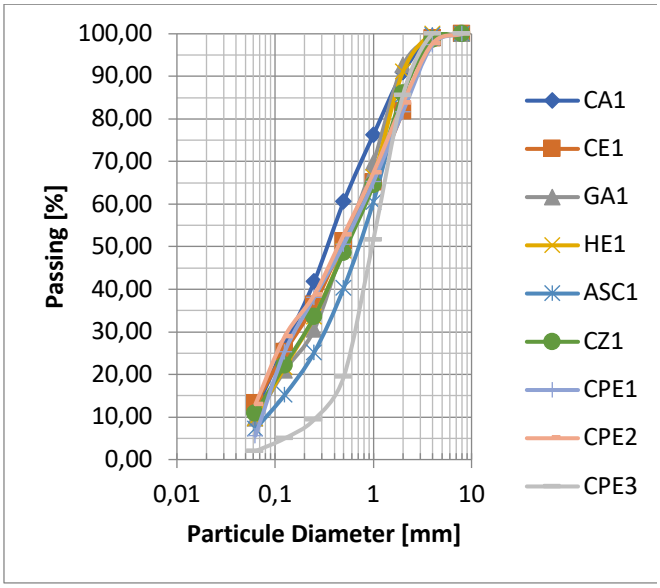

Figure 2 Particle size distribution of the aggregates.

Except the CPE3 sample, it is still possible to verify, through bigger aggregates macroscopic observation, that it has a mineralogic nature compatible with the local geology of Serra de Sintra. The macroscopic minerals visible are silicate, mainly of quartz and feldspathoid, and angulous in general. These aggregates may be associated to granitoids with pink tone or pinkish yellow that rise in the region.

The granulometric curve of CPE3 sample stands out from the others. The figure 2 shows the CPE3 mortar and allows to observe the presence of particles with grey, beige, and brown colour, and the absence of ceramic particles. The aggregates form is, in general, sub-rounded and rounded.

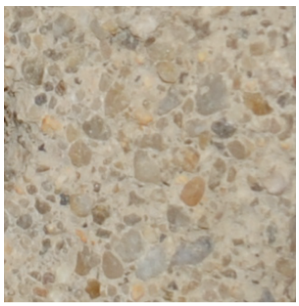

Figure 3 CPE3 mortar.

Comparing with the remaining samples, the studied aggregates do not present these characteristics neither do present minerals diversity, at least macroscopically visible. Their dimension was, in majority of the cases, thinner. The minimum diameter of the aggregates in the remaining samples was 0,063mm and this sample's diameter was the only one with higher dimensions. These disparities may, by hypothesis, be related to the fact that CPE3 sample was applied more recently and with more specific aggregates selected for it, which may even not be from the Convent surroundings.

3.3. Real density and porosity

Parameters values analyzed, namely porosity (P), real rensity (RD), 48 hours saturation (W_{48h}), maximum saturation ($W_{máx}$) and saturation coefficient (C_{sat}) can be seen on table 6.

The analysed samples revealed porosity values between 25 and 47%, The extreme values of porosity were obtained in CPE2 and CPE3. It matters to note that CA1 sample -value of 41%, being an indoor and unventilated space, presents identical values to CPE1 and CPE2 samples.

Table 7 Water behavior of mortar samples.

Sample	P [%]	RD [%]	W_{48H} [%]	$W_{máx}$ [%]	C_{sat} [%]
CPE1	43,5	1444	27,4	30,2	91
CPE2	45,8	1393	28,6	32,9	87
CPE3	25,5	1942	10,2	13,1	77
HE1	36,1	1660	17,1	21,7	79
ASC1	37,4	1621	20,1	23,2	87
CZ1	37,0	1627	20,8	22,8	91
CA11	41,1	1518	24,0	27,1	89
CE1	37,2	1630	20,1	22,8	88

The mortars revealed similar values of real density values ranging between 1393 kg/m^3 and 1942 kg/m^3. In this case, the sample with the highest real density is the one with the lowest porosity – CPE3. The other samples' results showed a regular trend. The porosity results are in line with historic mortars, as well as those for MVR. The values range may be related to several factors – soluble/insoluble residue relationship, aggregates granulometry, binder agglutinate properties, mixing water, and compactness (Sena da Fonseca et al., 2020).

The porosity value that most stands out refers to the CPE3 sample, which is substantially lower than the others, as well as its MVR value is also higher. This sample has characteristics that indicates it was a recently formulated and executed mortar compared to the others.

After 48 hours saturation, the highest porosity percentage were equally high in saturation. However, four samples – ASC1, CZ1, CA1 and CE1, with similar porosity values, presented saturation values above 20%. The detail was explained with the maximum saturation values obtained.

The C_{sat} analysis allows one to conclude that all the samples had high values for the saturation coefficient. CPE1 and CPE2 samples – 91% and 87%, respectively – denoted an inversion of the maximum values related to porosity. CPE3 presented a value of 77%, being the lowest sampling value.

3.4. Water absorption by Capillary

Table 8 presents the values of the coefficient of water absorption by capillarity of the studies mortars.

Table 8 Coefficients of water absorption by capillary.

Sample	Capillary Coefficient [kg/m^2.s^{0,5}]
CPE2	0,27
CPE3	0,11
HE1	0,18
ASC1	0,23
CZ1	0,23
CA1	0,65
CE1 (18)	0,18
CE1 (19)	0,34

Through the table analysis, one can highlight that HE1 and ASC1.A samples present very high porosity values. In fact, looking on the saturation coefficients, one can prove the higher value of ASC1.A, since this sample showed a C_{sat} of 88%, proving a higher water absorption capacity by capillarity.

CPE3 presented a lower coefficient in accordance with low porosity and saturation. It showed unforeseen values for an historic mortar since its values are lower than those referend in chapter 1.

Regarding CPE1, fragments of mortar were analysed firstly on the inside (interior) and, afterwards, the covering side (exterior). The aim was to verify if the covering had impermeabilization characteristics. The result may be observed in table 9.

Table 9 Coefficients of water absorption by capillary of different fragments of mortar that integrated the CPE1 sample

CPE1	Capillary Coefficient [kg/m^2.s^{0,5}]	
	Interior/mortar	**Exterior/coating**
Frag.1	0,35	0,18
Frag.2	0,24	0,43
Frag.3	0,35	0,17
Frag.4	0,23	0,12

The obtained values show that only fragment 2 did not presente a coefficient decrease with the covering existence. Also, one can denote that it is among the higher sampling figures.

Regarding fragments 3 and 4, the values are those expected for covering constituents, since it does not have lower coefficients than the mortar ones.

The coefficient of 0,12 kg/(m^2.s^{0,5}) in fragment 4 indicates, by hypothesis, that the covering led to a better behaviour when in contact with water, since it is the lowest value observed, excluding CPE3.

This way, it was possible to prove that the covering characteristics present in CPE1 did not address the desired impermeabilization to the samples. Since there were only punctual improvement, it was not enough for total sample extrapolation.

3.5. Colour characterization

3.5.1. Mortars

Figure 4 present the analysis mortars **C*** and **L*** values. One can infer that the highest points concentration in the abscises axys is between 15 and 20, while in the ordinate axys it is between 55 and 70. The samples with **L*** coordinate higher than 70 are CZ1 and ASC1. CPE2 sample has the particularity of having a **C*** coordinate higher than 20, it is placed in the yellow and orange spectrum. Lastly, the sample that is still different from others is CPE3, which its luminosity and chrome places it in grey colour.
In general, the samples present colour between beige and grey. In samples with **C*** higher than 20, the colour is situated in the yellow/brown, between the interval of 15 and 20, beige is the identified colour and values lower than 15, samples are closer to grey.

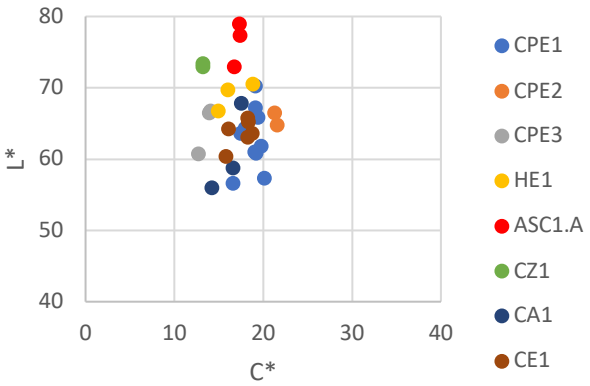

Figure 4 Graphic with.**C*** and **L*** mortar coordinates.

3.5.2. Decorative outer layer

Regarding coloration, as one can notice in figure 5, CZ1 samples diverges from others by presenting lower values in both coordinates. These results lead the colour for a dark grey colour, with a **C*** coordinate close to 10 and **L*** coordinate close to 50 – consonant with the real coating present in the sample.

CPE1 sample has an identic behaviour to those without coating. The luminosity coordinate set are higher to those on CZ1, between 15 and 20, as well as chrome ascended to 10. This way, its real colour approaches to beige.

Finally, CE1 showed average values on **C*** coordinate, identical to CZ1, but with the highest luminosity values. This conferred a light beige colour.

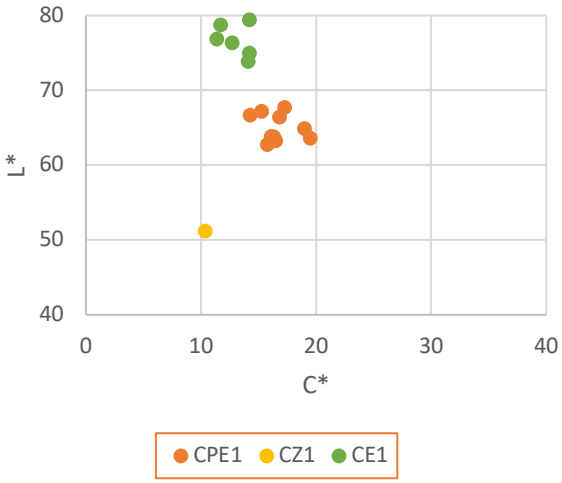

Figure 5 Graphic with.**C*** and **L*** coating coordinates.

4. Conclusions

The study was based on the lime mortars analysis, collected in situ. They were subject to a working methodology with the aim of assessing the physical characteristics, its behaviour in contact with water, composition, aggregate granulometry and estimating the approximate binder:aggregate ratio through the samples soluble/insoluble ratio analysis. The analyzed samples in this dissertation were collected in 9 places of Convento dos Capuchos, located along its 3 levels.

In the laboratory, the preparation of collected samples with photographic records was started before and after a cleaning adjusted on a case-by-case basis. At this stage, it was relevant to macroscopically evaluate characteristics inherent to each sample, regarding morphology, cohesion, voids, lime nodules presence, among others. This first phase was used to create a calibrated scale of physical parameters for the collected samples.

Regarding the characteristics of the aggregate used in the mortars' formulation, it was expected the use of granitic rocks typical of the region where the Convent's building is located. After samples dissolution with acid, the macroscopic evaluation of the insoluble fraction, it was possible to observe characteristics like the existing granite in Serra de Sintra.

HE1, CZ1, CE1 and ASC1.A samples revealed similar porosity values and capillary absorption coefficients, indicating the hypothesis that they were applied at the same time.

CPE1 and CPE2 samples showed similar absorption values to the previous group. However, with higher porosity.

CA1 and CPE3 samples stood out from the remaining ones, regarding their behaviour in contact with water. It should be noted that CPE3 presented itself as the sample with the best performance, presenting completely antagonistic values to those presented by the others and whose properties indicate that it was a more recently formulated repair mortar.

Regarding the mortars composition, the results are in line with other historical mortars already studied in Portugal. The trace values obtained, by analogy with the soluble and insoluble part previously described in this dissertation, refer to a range of values between 1:2 and 1:4. As an exception to these values, one can highlight the CPE3 sample, which results reflected a trace of 1:6.2, again distinct from the others.

Finally, in the three parameters combination that compose the CIELAB coordinates, the samples colour range can be represented by the samples CPE1, CZ1 and CE1: colours between brown, beige and grey. CZ1 samples shows however, a completely different hue from the rest, being the darkest of the specimens.

References

25-PEM - Protection et Érosion des Monuments, C. (1980a). *RILEM Test No. I.1 – Porosity accessible to water – Recommandations provisoires. Essais recommandés pour mesurer l'altération des pierres et évaluer l'éfficacité des methods de traitement*.

25-PEM - Protection et Érosion des Monuments, C. (1980b). *RILEM Test No. II.6 - Water Absorption Coefficient – Recommandations provisoires. Essais recommandés pour mesurer l'altération des pierres et évaluer l'éfficacité des methods de traitement*.

Aicher, P., Rowland, I. D., & Howe, T. N. (2001). Vitruvius: Ten Books on Architecture. In *The Classical World* (Vol. 94, Issue 3, p. 303). Harvard University Press. https://doi.org/10.2307/4352580

Almeida Santos, A. (2013). *Edifício da Central Tejo em Lisboa – Caraterização dos materiais e suas anomalias*. Instituto Superior Técnico.

Antunes, A. D. C., & Coroado, J. (2013). Characterization of Lime Mortars From an 18th Century River Tagus Quay (Lisbon, Portugal). *International Journal of Conservation Science*, *4*(1858), 515–524.

Appleton, J. (2011). *Reabilitação de Edifícios Antigos - Patologias e Tecnologias de Intervenção* (2º). Edições Orion.

Damas, A. L., Faria, P., & Veiga, R. (2016). *Caraterização de argamassas antigas de Portugal - Contributo para a sua correta conservação*. https://run.unl.pt/bitstream/10362/19316/1/CI - Damas et al_caract arg antigas_review_67_021_patrima2016.pdf

De Carvalho Antunes, A., Coroado, J., Santos Silva, A., & Veiga, R. (2016). *Estudo das argamassas do Cais das Colunas (Séc. XVIII), Lisboa, Portugal*. https://www.researchgate.net/publication/303645828

Ferreira Pinto, A. P., Sena da Fonseca, B., & Vaz Silva, D. (2020). The role of aggregate and binder content in the physical and mechanical properties of mortars from historical rubble stone masonry walls of the National Palace of Sintra. *Construction and Building Materials*. https://doi.org/10.1016/j.conbuildmat.2020.121080

Garijo, L., Zhang, X. X., Ruiz, G., Ortega, J. J., Real, C., & Real, C. (2020). *The influence of dosage and production process on the physical and mechanical properties of air lime mortars*. *XLIV*(September), 9–12.

Gomes, A., Pinto, A. P., & Pinto, J. B. (2013). *Gesso e cal de construção*. 5–12. https://fenix.tecnico.ulisboa.pt/downloadFile/3779580050974/Gesso e Cal_2013.pdf

Groot, C. (2005). *1. Characterisation of Old Mortars With Respect To Their Repair: a State of the Art. 1*(i), 1–10. https://doi.org/10.1617/2912143675.001

Huaracha, Y. (2018). *Influência do agregado calcário em argamassas para rebocos de substituição de edifícios antigos*. Instituto Superior Técnico.

Lezzerini, M., Legnaioli, S., Lorenzetti, G., Palleschi, V., & Tamponi, M.

(2014). Characterization of historical mortars from the bell tower of St. Nicholas church (Pisa, Italy). *Construction and Building Materials*, *69*, 203–212. https://doi.org/10.1016/j.conbuildmat.2014.07.051

Margalha, M. G., Veiga, R., & Brito, J. de. (2007). Influência das areias na qualidade de argamassas de cal aérea. *2º Congresso Nacional de Argamassas De Construção, Lisboa, PORTUGAL*.

Minolta, K. (2014). *Problems with CIE Lab (L*a*b* color space) - Part V - Precise Color Communication | KONICA MINOLTA*. Retrieved November 5, 2020, from https://www.konicaminolta.com/instruments/knowledge/color/part5/01.html

Nogueira, R., Pinto, A. P., & Gomes, A. (2016). *Rebocos à base de cal: passado e presente Conhecimento empírico versus conhecimento científico. 1*.

Rosa, P. J. P. da. (2016). *Caracterização de argamassas históricas do Convento de Cristo - Tomar*. https://repositorio.ul.pt/handle/10451/25618?locale=en

Scannell, S., Lawrence, M., & Walker, P. (2014). Impact of aggregate type on air lime mortar properties. *Energy Procedia*, *62*(November 2015), 81–90. https://doi.org/10.1016/j.egypro.2014.12.369

Sena da Fonseca, B., Ferreira Pinto, A. P., & Vaz Silva, D. (2020). Compositional and textural characterization of historical bedding mortars from rubble stone masonries: Contribution for the design of compatible repair mortars. *Construction and Building Materials*, *247*. https://doi.org/10.1016/j.conbuildmat.2020.118627

UNESCO. (1995). *Cultural Landscape of Sintra - UNESCO World Heritage Centre*. Retrieved March 5, 2019, from https://whc.unesco.org/en/list/723/

Veiga, R. (2006). *Os revestimentos antigos e a identidade dos edifícios. Arquitectura Ibérica. Reabilitação. N.12*. http://conservarcal.lnec.pt/pdfs/RV_ArqIber.pdf

Veiga, R. (2009). Conservação e Reparação de Revestimentos De Paredes De Edifícios Antigos - Métodos e Materiais. In *Teses e Programas de Investigação, LNEC, Lisboa*. www.lnec.pt

Veiga, R. (2017). Air lime mortars: What else do we need to know to apply them in conservation and rehabilitation interventions? A review. *Construction and Building Materials*, *157*, 132–140. https://doi.org/10.1016/j.conbuildmat.2017.09.080

Veiga, R. (2018). Argamassas de cal para conservação e reabilitação de edifícios: conhecimento consolidado e necessidades de investigação. *Ambiente Construído*, *18*(4), 85–96. https://doi.org/10.1590/s1678-86212018000400295